

Effect of Fly Ash Deposit on Thermal Performance of Spiral Finned-Tube Heat Exchanger under Dehumidifying Condition

Atipoang Nuntaphan^{1*} and Tanongkiat Kiatsiriroat²

¹*Thermal Technology Research Laboratory, Mae Moh Training Center, Electricity Generating Authority of Thailand, Mae Moh, Lampang 52220, Thailand*

²*Department of Mechanical Engineering, Faculty of Engineering, Chiang Mai University, Chiang Mai 50200, Thailand*

*Corresponding author. E-mail: atipoang.n@egat.co.th

ABSTRACT

This research investigated the effect of fly ash deposit on thermal performance of a cross-flow heat exchanger, having a set of spiral finned tubes as heat transfer surface. A stream of warm air having high content of fly ash was exchanging heat with a cool water stream in the tubes. In this study, the temperature of the heat exchanger surface was lower than the dew point temperature of air, thus there was condensation of moisture in the air stream on the heat exchanger surface. The affecting parameters such as the air mass flow rate, the fly ash mass flow rate and the inlet temperature of warm air were varied while the volume flow rate and the inlet temperature of the cold water stream were kept constant at 10 l/min and 5°C, respectively.

From the experiment, it was found that the thermal resistance due to the fouling increased with time. Moreover, the deposit of fly ash on the heat transfer surface was strongly dependent on the air-ash ratio and the amount of condensate on the heat exchanger surface. The empirical model for evaluating the thermal resistance was also developed in this work and the simulated results were found to agree quite well with those of the measured data.

Key words: Particulate fouling, Heat exchanger testing, Thermal resistance

INTRODUCTION

Heat exchanger is an equipment for recovering heat from the waste heat source. For recovering waste heat from flue gas, the cross-flow heat exchanger type is commonly used. Normally, this kind of heat exchanger faces with the particulate from flue gas which usually deposits on the heat transfer surface. Because of the low thermal conductivity of the fouling material, the thermal performance of heat exchanger is therefore decreased.

Many researchers try to explain the fouling phenomenon of the heat transfer surface and develop many correlations for predicting the thermal resistance due to fouling. One well-known model for evaluating the thermal resistance of fouling

was developed by Kern and Seaton (1959). This model verified the asymptotic behavior of the deposit formation on the surface. Kim and Kim (1992) studied the particulate fouling on the circular cylinder in high temperature laminar cross flow. Kaiser et al., (2002) carried out the experiment to study the formation of fouling layers on cylindrical tube under warm, humid and solid-loaded air. Abd-Elhady et al., (2004) investigated the influence of gas velocity in the heat exchanger to avoid the particulate fouling. Bouris and Bergeles (1997) and Bouris et al., (2001) used the numerical method for calculating the efficiency of heat exchanger under fouling and evaluated the effect of tube configuration on the particulate fouling.

Very few reports have been presented in case of heat exchanging of warm, humid air with high particulate. Therefore, the objective of this work was to investigate the performance of spiral finned-tube bank with particulate fouling from fly ash under dehumidifying condition. The results of this work can be used for the design of the heat recovery unit of the flue gas having high particulate such as the coal-fired boiler.

MATERIALS AND METHODS

Figure 1 shows the schematic presentation of the experimental apparatus. In this study, the cross-flow heat exchanger using spiral finned tubes was considered because this kind of heat exchanger is commonly used for recovering heat from flue gas. The dimensions of the heat exchanger are given in Table 1.

In this experiment, the ambient air was fed by a 1.5 kW centrifugal air blower in a wind tunnel through an electric heater for generating hot air. The temperature could be controlled by a temperature controller. The hot air was mixed with fly ash fed from a dust feeder. Note that, the diameter of fly ash was lower than $40\ \mu\text{m}$. The air-dust mixture was flowing through the tube bank and exchanging heat with cold water, circulation inside the tubes. In this work, the volume flow rate and the inlet temperature of the cold water were kept constant at 10 l/min and 5°C , respectively.

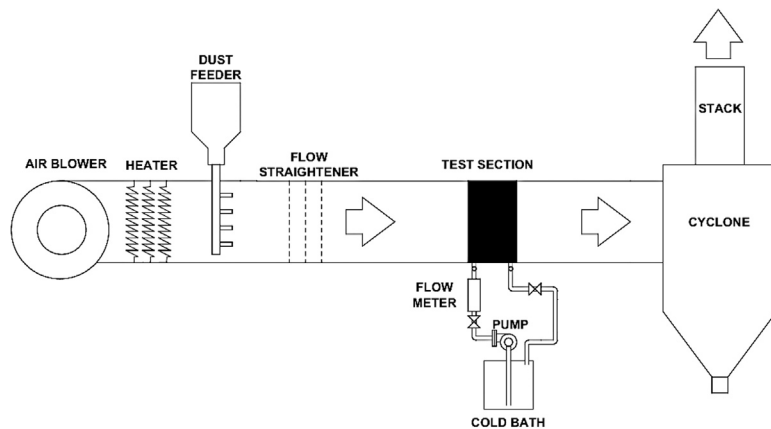


Figure 1. Schematic presentation of the experimental setup.

Table 1. Geometrical parameters of the heat exchanger.

Item	Detail
Type of heat exchanger	Cross-flow
Number of row	4
Number of tube in each row	8
Tube outer diameter	2.17 cm
Tube length	45.0 cm
Tube thickness	2.6 mm
Tube arrangement	Staggered
Transverse tube pitch	5.56 cm
Longitudinal tube pitch	4.82 cm
Type of fin	Spiral
Fin height	10.0 mm
Fin spacing	3.85 mm
Fin thickness	0.40 mm

Table 2. Testing conditions.

Item	Detail
Mass flow rate of air	0.14–0.26 kg/s
Mass flow rate of fly ash	0–0.006 kg/s
Volume flow rate of water	10 l/min
Inlet temperature of air-dust mixture	40, 60°C
Inlet temperature of water	5°C
Testing interval	8 hr

The inlet and outlet temperatures of the air-dust mixture and the water were measured by a set of K-type thermocouples with an accuracy of $\pm 0.1^\circ\text{C}$. The mass flow rate of the air stream was measured by a hot-wire anemometer with an accuracy of ± 0.01 m/s. An accurate flow meter was used for measuring the water flow rate with an accuracy of ± 0.1 L/min. The testing conditions are shown in Table 2.

DATA REDUCTION

In this work, the effect of fly ash deposit on the heat exchanger performance was studied via the thermal resistance of fouling.

During the experiment, the heat transfer rate of a heat exchanger (Q) could be calculated from the water side as:

$$Q = m\dot{m}_w C_{p_w} (T_{wo} - T_{wi}) \quad (1)$$

Where $m\dot{m}_w$ is the mass flow rate of water; T_{wi} , T_{wo} are the inlet and outlet temperature of water, and C_{p_w} is the specific heat of water.

The heat transfer rate of the heat exchanger can also be calculated from the bulk temperature difference of both fluids as:

$$Q = (UA)(T_a - T_w) \quad (2)$$

Where U and A are overall heat transfer coefficient and area of the heat exchanger; T_a and T_w are bulk temperatures of the air-dust mixture and the water, respectively.

The total thermal resistance due to the overall heat transfer coefficient and the area in Eq. (2) can be calculated by:

$$\frac{1}{UA} = Z_o + \frac{\ln(d_o/d_i)}{2\pi kL} + \frac{1}{h_i A_i} + Z_f \quad (3)$$

h_i is the tube-side heat transfer coefficient; A_i is the inner surface area of the heat exchanger; d_i and d_o are the inner and the outer tube diameters, respectively; L is the total tube length; k is the thermal conductivity of tube material; Z_o is the air-side thermal resistance; Z_f is defined as the thermal resistance due to fouling of fly ash on the external surface of heat exchanger.

The inner heat transfer coefficient can be calculated from Gnielinski correlation (1976) as:

$$h_i = \left(\frac{k}{d} \right)_i \frac{(Re_{Di} - 1000) Pr(f_i/2)}{1 + 12.7 \sqrt{f_i/2} (Pr^{2/3} - 1)}, \quad (4)$$

$$f_i = [1.58 \ln(Re_{Di}) - 3.28]^2, \quad (5)$$

where Re_{Di} is the tube-side Reynolds number.

The air-side thermal resistance, Z_o , can be evaluated from Eqns (2) and (3) when the heat exchanger is clean (no dust condition).

RESULTS AND DISCUSSION

Figure 2 shows the heat transfer deterioration with time of the heat exchanger due to fouling from fly ash. In this case, the inlet temperature of the air-dust mixture was at 40°C. It was found that the ratio of the heat transfer of the heat exchanger with fouling and that with clean condition (at $t=0$) decreased with time lapse. It could also be seen that the heat transfer deterioration depended on the ratio of air and dust, x ($x = m\dot{m}_d / m\dot{m}_a$), in the mixture. When x was increased, higher fouling was obtained which resulted in lower heat transfer rate.

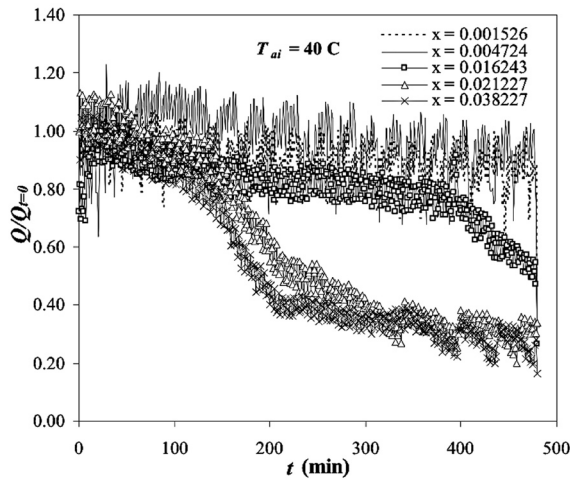


Figure 2. The deterioration of heat transfer at various times in case of $T_{ai} = 40^{\circ}\text{C}$.

However, from Figure 2, it was found that at the first stage of fouling ($t < 50$ min, approximately), the heat transfer rate tended to be higher than that of the clean condition, especially at low x value. As the deposit layer built up, the flow area of air was decreased which resulted in higher air velocity. Moreover, the fouling layer was likely to be rougher than the clean surface. Therefore, the air-side heat transfer coefficient should be increased. But when the thickness of the fouling layer was developed further, the effect of low thermal conductivity of the fouling dominated the previous enhancement result. Therefore, the heat transfer performance of the heat exchanger was then decreased. This phenomenon was first reported by Gudmundsson and Bott (1979) who studied the deposition of silica on a geothermal heat exchanger.

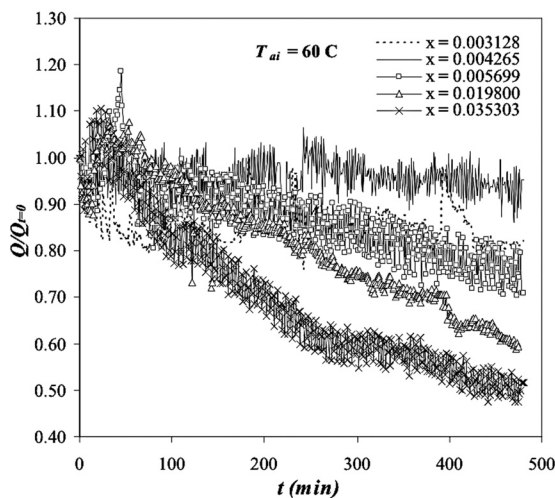
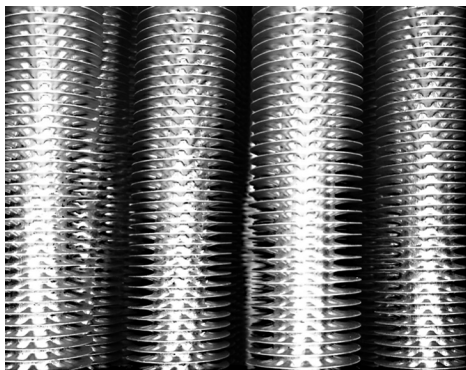


Figure 3. The deterioration of heat transfer at various times in case of $T_{ai} = 60^{\circ}\text{C}$.

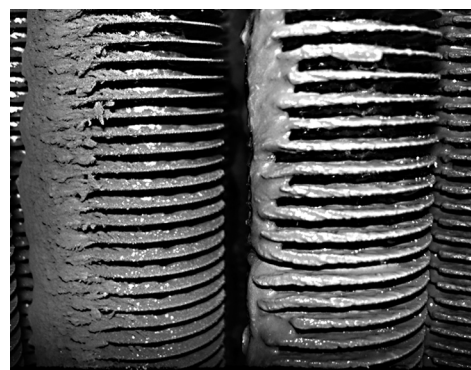
Figure 3 also shows the same result as Figure 2. The inlet air temperature was kept constant at 60°C. Since the surface temperature of the heat exchanger was lower than the dew point temperature, consequently, the condensation of moisture in the air on the heat transfer surface occurred. For $T_{ai} = 40^\circ\text{C}$, lower heat rate was needed for extracting heat from the air to get condensed, thus the surface of the heat exchanger was wetter than that of $T_{ai} = 60^\circ\text{C}$. The condensate could have promoted the adhesion of particles onto the heat transfer surface and higher heat transfer deterioration was thus obtained. It could be seen that, in case of $T_{ai} = 40^\circ\text{C}$, the deterioration of heat transfer tended to be higher than that of $T_{ai} = 60^\circ\text{C}$, especially at high fly ash content. Consequently, the heat exchanger having $T_{ai} = 40^\circ\text{C}$ had lower heat transfer rate than that of $T_{ai} = 60^\circ\text{C}$.

Figure 4 shows the formation of fly ash on the heat transfer surface at various conditions and compares with that of the clean surface. Figures 4b and 4c show the cases of $x = 0.016$, $t = 4$ hr, $T_{ai} = 40^\circ\text{C}$ and $x = 0.016$, $t = 8$ hr, $T_{ai} = 40^\circ\text{C}$, respectively. Compare Fig. 4c with Fig. 4d ($x = 0.036$, $t = 8$ hr, $T_{ai} = 40^\circ\text{C}$), it was found that the forming of fly ash increased with the dust content in the air stream. Figures 4d and 4e ($x = 0.036$, $t = 8$ hr, $T_{ai} = 60^\circ\text{C}$) show the effect of the inlet air temperature on the fouling deposit. The data of the fouling forming also confirmed the heat transfer phenomenon in Figures 2-3.

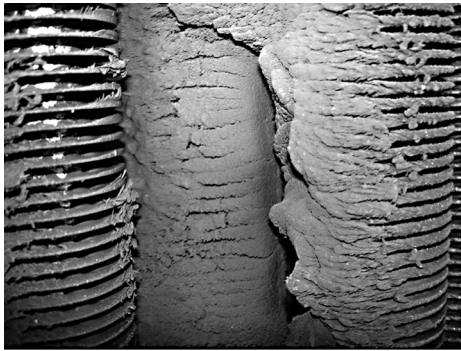
Following the direction of air flow (from left to right), all pictures in Figure 4 show the deposition of fly ash particles at the front part of the tube. The results differed from the work of Kaiser et al., (2002) and Abd-Elhady et al., (2004) who studied the deposit of particles on cylindrical tubes. They found that the formation of foulant occurred mostly at the rear part of the cylindrical probes. In this experiment, the finned-tube surface was wetted, therefore, the attractive force between the particles and the surface was higher than that of the dry surface. Thus, most of the particles were attached to the front part of the finned tube.



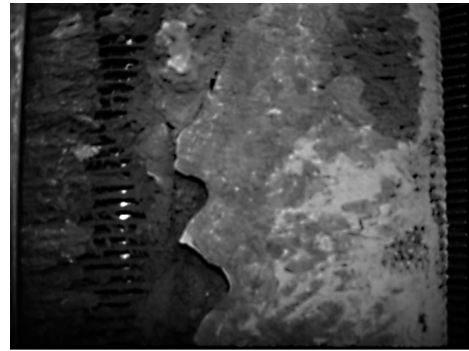
a. Clean surface heat exchanger



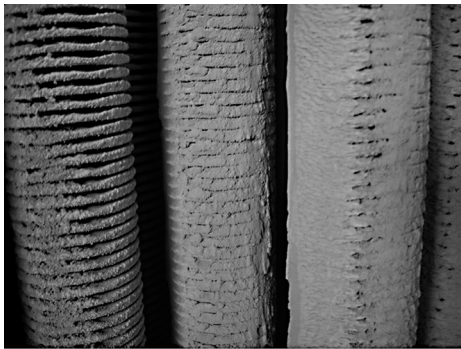
b. $x = 0.016$, $t = 4$ hr, $T_{ai} = 40^\circ\text{C}$



c. $x = 0.016, t = 8 \text{ hr}, T_{ai} = 40^\circ\text{C}$



d. $x = 0.036, t = 8 \text{ hr}, T_{ai} = 40^\circ\text{C}$



e. $x = 0.036, t = 8 \text{ hr}, T_{ai} = 60^\circ\text{C}$

Figure 4. Fouling from fly ash on heat exchanger surface at various conditions.

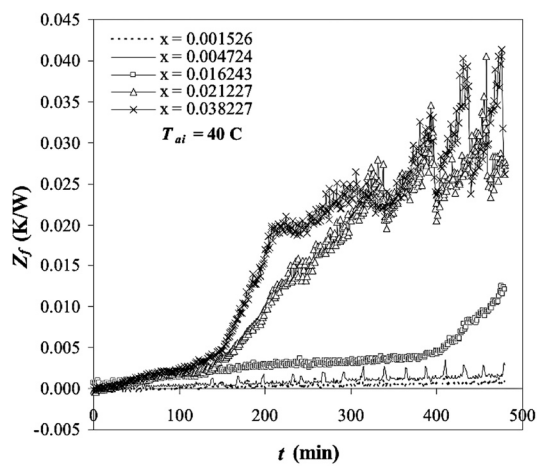


Figure 5. The thermal resistance of heat transfer at various times in case of $T_{ai} = 40^\circ\text{C}$.

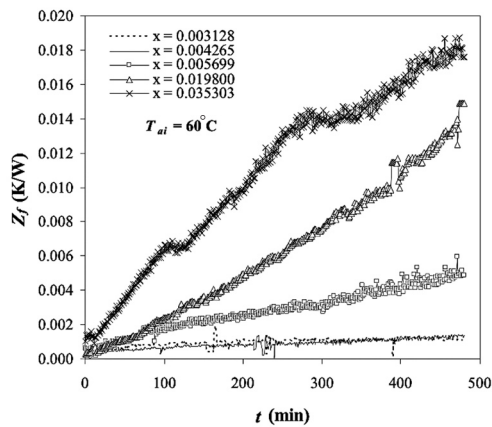


Figure 6. The thermal resistance of heat transfer at various times in case of $T_{ai} = 60^{\circ}\text{C}$.

Figures 5-6 show the thermal resistance of the heat exchanger in case of $T_{ai} = 40^{\circ}\text{C}$ and 60°C , respectively. Similar to the results in Figures 2-3, the thermal resistance increased with time and x value. Moreover, the effect of lower inlet temperature of the air stream tended to promote higher thermal resistance, especially at high dust content condition.

In this research, the correlation for predicting the thermal resistance of the heat exchanger under fouling and dehumidifying conditions was also developed. Although Kern and Seaton (1959) proposed a well known asymptotic model for evaluating the thermal resistance as:

$$Z_f = Z_a(1 - e^{-\beta t}). \quad (6)$$

Z_f is thermal resistance due to fouling at a specified time; Z_a is thermal resistance at the asymptotic point; t is time and β is empirical constant. To get the thermal resistance at the asymptotic point, a lot of experiments and time are needed. Therefore, in this work, a set of correlations for predicting the thermal resistance was developed from the experimental data as:

$$\frac{Z_f}{Z_{clean}} = 366.45\tau^a x^b \delta^c, \quad (7)$$

$$\tau = \frac{T_{ai} - T_{dew}}{T_{ai} - T_{wi}}, \quad (8)$$

$$x = \frac{m\&_d}{m\&_a}, \quad (9)$$

$$\delta = \frac{t}{t_{total}} , \tag{10}$$

$$a = 1.3927 + 40.3590x - 1.2777\delta , \tag{11}$$

$$b = 1.2521, \tag{12}$$

$$c = -0.3081 + 24.7480x + 0.7124\tau . \tag{13}$$

Where Z_{clean} is thermal resistance of the heat exchanger at clean condition; T_{dew} is the dew point temperature of the inlet air; and are time and total experimental time lapse (8 hr), respectively; t and t_{total} are mass flow rate of dust and air, respectively.

Figure 7 shows the predicted thermal resistance ratio and 80% of the experimental data could be fitted by the correlation within 20% error.

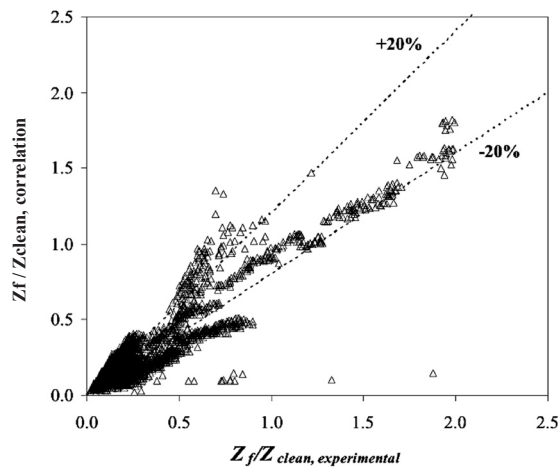


Figure 7. The comparison of thermal resistance ratio from experimental data and correlation.

CONCLUSION

From this experiment, it can be concluded that the fouling of finned-tube heat exchanger under dehumidifying condition depended on the air-dust content and the inlet temperature of air stream. The formation of foulant occurs mostly on the front part of finned tubes.

The developed empirical model could be used to predict the thermal resistance due to the fouling and the results seen to agree quite well with the experimental data.

ACKNOWLEDGEMENTS

The authors gratefully acknowledge the financial support provided by the Thailand Research Fund for carrying out this investigation.

REFERENCES

- Abd-Elhady, M.S., C.C.M. Rindt, J.G. Wijers, A.A.V. Steenhoven, E.A. Bramer, and T.H.V.D. Meer. 2004. Minimum gas speed in heat exchangers to avoid particulate fouling. *International Journal of Heat and Mass Transfer* 47 : 3943-3955.
- Bouris, D., and G. Bergeles. 1997. Numerical calculation of the effect of deposit formation on heat-exchanger efficiency. *International Journal of Heat and Mass Transfer* 40 : 4073-4084.
- Bouris, D., G. Papadakis, and G. Bergeles. 2001. Numerical evaluation of alternate tube configurations for particle deposition rate reduction in heat exchanger tube bundles. *Journal of Heat and Fluid Flow* 22 : 525-536.
- Gnielinski, V. 1976. New equation for heat and mass transfer in turbulent pipe and channel flow. *International Chemical Engineering* 16 : 359-368.
- Gudmundsson, J.S., and T.R. Bott. 1979. Deposition of silica from geothermal waters on heat transfer surfaces. *Desalination* 28 : 125-145.
- Kaiser, S., D. Antonijevic, and E. Tsotsas. 2002. Formation of fouling layers on a heat exchanger element exposed to warm, humid and solid loaded air stream. *Experimental Thermal and Fluid Sciences* 26 : 291-297.
- Kern, D.Q., and R.E. Seaton. 1959. A theoretical analysis of thermal surface fouling. *Brit. Chemical Engineering* 4 : 258.
- Kim, Y.J., and S.S. Kim. 1992. Experimental study of particle deposition onto a circular cylinder in high-temperature particle laden flows. *Experimental Thermal and Fluid Sciences* 5 : 116-123.

NOMENCLATURE

A	Area (m ²)
A_i	Internal area of tube (m ²)
A_o	External area of tube (m ²)
Cp_w	Specific heat of water (J/kgK)
d_i	Inner diameter of tube (m)
d_o	Outer diameter of tube (m)
h_i	Tube-side heat transfer coefficient (W/m ² K)
k	Thermal conductivity of tube material (W/mK)
L	Total tube length (m)
$m\&_a$	Mass flow rate of air (kg/s)
$m\&_d$	Mass flow rate of dust (kg/s)
$m\&_w$	Mass flow rate of water (kg/s)
Q	Heat transfer rate of a heat exchanger (W)

t	Time (hr)
T_a	Bulk temperature of air (°C)
T_{ai}	Inlet temperature of air (°C)
T_{dew}	Dew point temperature of air (°C)
T_w	Bulk temperature of water (°C)
T_{wi}	Inlet temperature of water (°C)
T_{wo}	Outlet temperature of water (°C)
U	Overall heat transfer coefficient (W/m ² K)
x	Ratio of air-dust mixture
Z_a	Asymptotic thermal resistance due to fouling (K/W)
Z_{clean}	Thermal resistance of clean heat exchanger (K/W)
Z_f	Thermal resistance due to fouling (K/W)
Z_o	Air-side thermal resistance (K/W)
δ	Dimensionless term of time
τ	Dimensionless term of temperature